Appendix 1 Detailed imaging protocols for CT and MRI scans

CT scans were performed using GE Discovery CT 750 HD Gemstone Spectral CT and Revolution EVO CT, as well as Philips' Brilliance iCT scanner. Patients were placed in a supine position with the scanning range covering the entire liver. The scanning parameters were as follows: tube voltage of 120 kV or rapid switching between 80/140 kV, tube current of 200–400 mA, field of view (FOV) ranging from 36 cm × 36 cm to 40 cm × 40 cm. The slice thickness and spacing were both 5 mm, with a pitch of 1.375:1 and a rotation time of 0.35–1.0 s/rotation. After obtaining the raw images, thin-slice reconstruction and multiplanar reformation were carried out. For contrast-enhanced scanning, iodixanol (containing 350 mg/mL iodine, GE Healthcare (Shanghai) Co., Ltd.) or iopamidol injection (containing 370 mg/mL iodine, BeiLu Pharmaceutical Co., Ltd., Beijing, China) was administered via the antecubital vein at a dose of 80–100 mL with an injection rate of 2.5–3 mL/s. Scanning was performed at delay times of 25–30, 46–60, and 100–150 s to obtain arterial, portal venous, and equilibrium phase images.

MRI scans were conducted using Philips' Achieva 3.0 T MRI and Siemens' Prisma 3.0 T MRI and Skyra 3.0 T MRI scanners, equipped with 16- or 18-channel body coils. Patients were positioned supine with the scanning range extending from the diaphragmatic dome to the lower poles of both kidneys. The scanning sequences and parameters were as follows: (I) axial T2WI using a fast spin-echo sequence (respiration-triggered) with TR of 3000–4000 ms and TE of 80–90 ms; (II) axial T1WI using a fast gradient-echo water-fat in-phase and opposed-phase sequence (breath-hold) with TR of 100–200 ms, TE in-phase of 2.2–2.6 ms, and TE opposed-phase of 1.1–1.3 ms; (III) Coronal T2WI using a single-shot fast spin-echo sequence (breath-hold) with TR of 3,000–5,000 ms and TE of 80–90 ms; (IV) axial DWI using a single-shot echo-planar imaging sequence (respiration-triggered) with b-values of 0 and 800 s/mm2 or 1,000 s/mm2, TR of 5,000–7,000 ms, and TE of 60–80 ms. All sequences had a slice thickness of 6–8 mm, slice spacing of 0–1 mm, FOV of 36 cm × 36 cm to 40 cm × 40 cm, and matrix sizes ranging from 256×225 to 320×256. For contrast-enhanced scanning, a three-dimensional volumetric interpolated breath-hold T1WI gradient-echo sequence was used with TR of 3–5 ms and TE of 1–2 ms. Contrast agents included gadopentetate dimeglumine (Gd-DTPA, concentration 0.5 mmol/mL, BeiLu Pharmaceutical, Beijing, China; injection dose of 0.1 mmol/kg, flow rate 2–3 mL/s) and the hepatocyte-specific contrast agent gadobenate dimeglumine (Gd-EOB-DTPA, mass concentration 181.43 mg/mL, Bayer; injection dose 0.1 mL/kg, flow rate 3–4 mL/s). After intravenous injection via the antecubital vein, images were acquired at delay times of 20–25 s, 46–60 s, 2–3 min, and 20 min to obtain arterial, portal venous, equilibrium (transitional) phase, and hepatobiliary phase images.

https://dx.doi.org/10.21037/qims-2025-1-2595

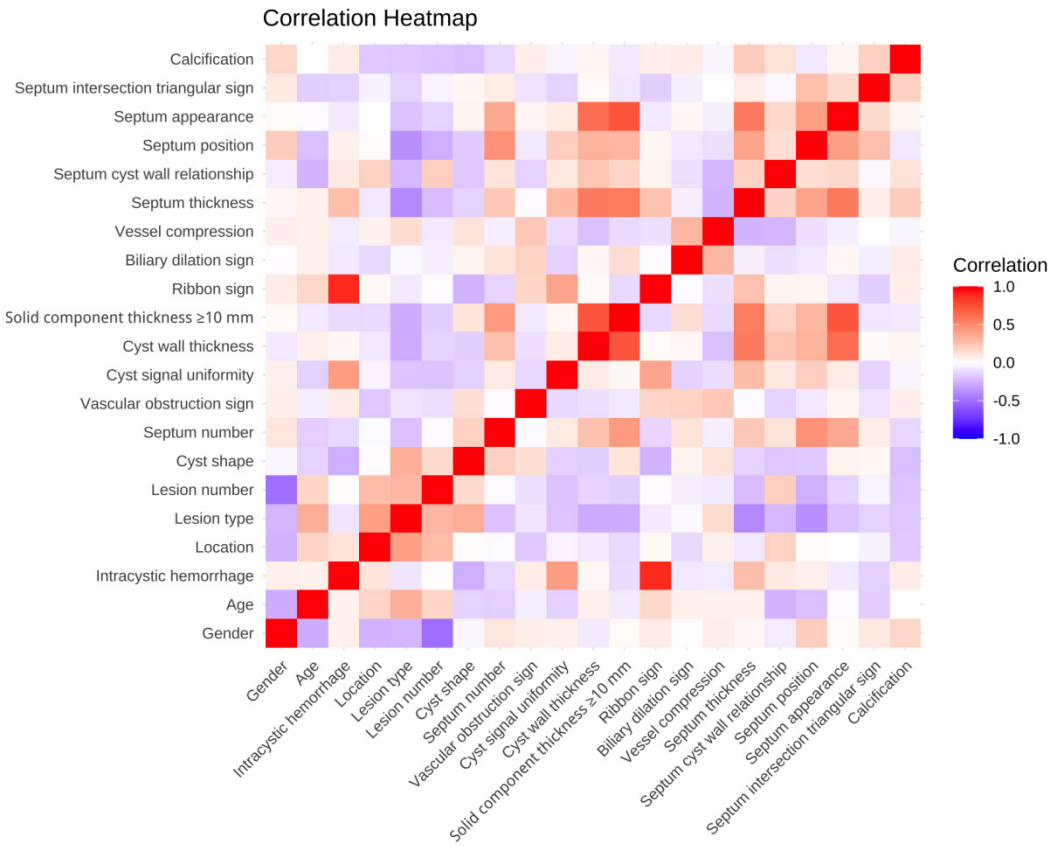

Figure S1 Heat map of correlation coefficient. The correlation between variables is calculated using the Spearman correlation coefficient method. Pairs of variables with a correlation coefficient absolute value greater than 0.8 are considered to have multicollinearity issues.

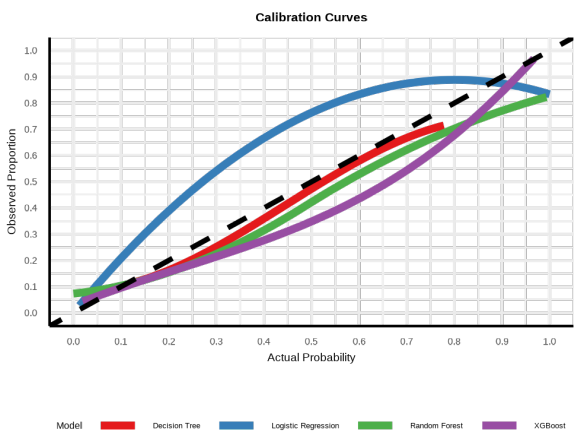

Figure S2 Calibration curve for the models incorporating six indicators. The x-axis indicates the predicted probability of disease presence, and the y-axis shows the actual observed proportion. All models exhibit calibration curves close to the diagonal line, signifying a good match between prediction and reality.

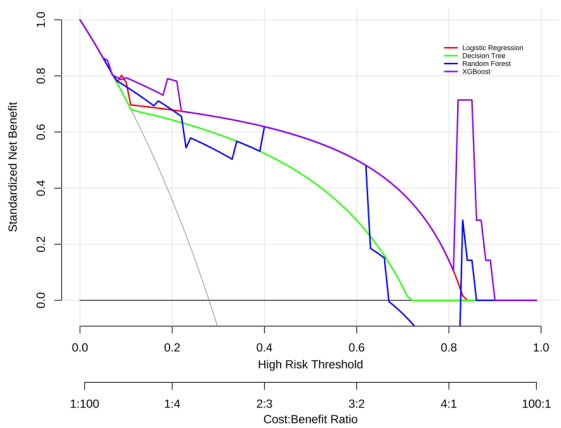

Figure S3 Decision curve analysis curves for the models incorporating six indicators. The x-axis represents the high-risk threshold probability, while the y-axis shows the standardized net benefit. The purple line, representing the XGBoost model, demonstrates superior net benefit over a range of threshold probabilities, suggesting its enhanced clinical applicability in distinguishing between MHC and MCN.

https://dx.doi.org/10.21037/qims-2025-1-2595